Settling velocity of equiaxed dendrites in a tube*

Zhou Peng(周 鹏), Wang Meng(王 猛)†, Lin Xin(林 鑫), and Huang Wei-Dong(黄卫东)

State Key Laboratory of Solidification Processing, Northwestern Polytechnical University, Xi'an 710072, *China*

(Received 8 August 2012; revised manuscript received 31 October 2012)

The settling velocity of equiaxed dendrites can cause macrosegregation and influence the structure of the equiaxed zone during the casting solidification process. So an understanding of the settling characteristics is needed to predict the structure and segregation in castings. The settling velocity of NH_4Cl equiaxed dendrites of non-spherical geometry was studied experimentally in an NH_4Cl–70wt.%H_2O solution. A calculation formula was proposed to calculate the settling velocity of sediment equiaxed dendrites in a tube filled with saturated solution at a moderate Reynolds number region. The retardation effects of the wall and morphology of the equiaxed dendrite on the settling velocity were taken into account in the development of the calculation formula, and the correction function B of the drag coefficient with consideration of the retardation effects of the wall and morphology of the equiaxed dendrite on the settling velocity of the equiaxed dendrite was calibrated according to the experimental results. A comparison showed that the formula has a good accordance with the experimental results.

Keywords: equiaxed dendrite, settling velocity, morphology effect, wall effect

PACS: 81.05.Bx, 47.50.Cd, 47.57.ef **DOI:** 10.1088/1674-1056/22/1/018101

1. Introduction

Free equiaxed dendrites are frequently observed in melts, growing from heterogeneous nucleation, fragmented dendrite arms, or initial nucleation on the mold wall or melt surface.[1–4] The sedimentation of equiaxed dendrites in a melt due to a density difference has been considered as an important reason for the formation of microstructure distribution and macrosegregation in metal castings,[5] unless solidification is performed in microgravity conditions.[6] Therefore, it is very important to evaluate the settling velocity of equiaxed dendrites for understanding and optimal control of the solidification process.

The settling behavior of equiaxed dendrites in a melt has been widely studied, and most of the work dealt with the estimation of the drag force and proposed related formulas to calculate the settling velocity. Stokes' law[7] has been used by Allen and Weinberg to analyze the settling process of equiaxed dendrites.[8,9] However obvious errors were shown in their results. It has been proposed that a highly non-spherical morphology of the equiaxed dendrite may contribute to this deviation.[10] Later, Zakhem *et al*. calculated the drag force for a settling equiaxed dendrite and examined the effects of dendrite geometry on the settling velocity[11] with a hypothesis that the interdendritic liquid of equiaxed dendrites was effectively immobilized and the additional surface area of the secondary dendrite arms has no influence on the drag coefficient of the dendrite. The concept of a dendrite envelope was proposed by Ahuja *et al.*,[12] and the fluid flow around the dendrite envelope was estimated, which imposed an effect on the drag force and the settling velocity of the equiaxed dendrite. By the efforts of Zakhem and Ahuja, the morphological effects on the sedimentation, together with the corrections for wall and inertial effects, were included in the approach for real experimental situations. However, those calculation formulas can only be applied to low Reynolds numbers ($Re \leq 1$). Recently, a calculation formula was put forward by Mirihanage *et al.* to estimate the settling velocity of an isolated equiaxed dendrite in a viscous fluid at a moderate Reynolds number region ($1 \leq Re \leq 100$) by using a drag coefficient corrected with the Reynolds number and a factor introduced to account for the effect of shape on drag forces.[13] However, they ignored a more important fact that confining walls or finite boundaries exerted a great extra retardation force on freely equiaxed dendrites settling in a vessel filled with fluid. The retardation effect of the wall on drag force should have been taken into account.

In this work, experimental results on the settling velocity of an NH_4Cl equiaxed dendrite settling in a tube filled with saturated NH_4Cl–70wt.%H_2O solution at a moderate Reynolds number region were reported. A new calculation formula was proposed for the moderate Reynolds number region ($1 \leq Re \leq 100$). The retardation effects of the tube wall and the shape of equiaxed dendrites were taken into account in the development of the calculation formula. Finally, a correction function B that incorporated the additional drag force effects of real dendrite shape and wall retardation was assessed.

*Project supported by the National Basic Research Program of China (Grant No. 2011CB10402), the National Natural Science Foundation of China (Grant Nos. 50901061 and 50971102), and the Foundation of State Key Laboratory of Solidification Processing, China (Grant Nos. 02-TZ-2008 and 36-TP-2009).

†Corresponding author. E-mail: wangmeng@nwpu.edu.cn

© 2013 Chinese Physical Society and IOP Publishing Ltd

2. Calculation formulas

The settling velocity changes to a constant when the net gravitational force (gravity minus buoyancy) equals the drag force.[14] This can be written as

$$W - B_{\mathrm{u}} = D_{\mathrm{r}}, \tag{1}$$

where W is the weight of a particle, B_{u} is the buoyancy of the particle, and D_{r} is the drag force on the particle. If the particle is a solid sphere, the net gravitational force is given by

$$W - B_{\mathrm{u}} = \pi(\rho_{\mathrm{s}} - \rho)g\frac{d^3}{6}, \tag{2}$$

where ρ_{s} is the density of the solid sphere, ρ is the density of the liquid, and d is the diameter of the settling sphere. The drag force that acts on the moving particle can be written as[15]

$$D_{\mathrm{r}} = \frac{1}{2}C_{\mathrm{d}}\rho A v^2, \tag{3}$$

where C_{d} is the drag coefficient, v is the settling velocity of the particle in liquid, and A is the projection area of the moving object perpendicular to the direction of movement.

Due to the liquid inertial effect on the velocity of a spherical particle,[16] the drag coefficient cannot be predicted theoretically, and is estimated by using empirical formulas with dependence on the Reynolds number of the spherical particle. One of the most widely used empirical equations was presented by Olson,[17] which was expressed as

$$C_{\mathrm{d}} = \frac{24}{Re}\left(1 + \frac{3}{16}Re\right)^{1/2}, \tag{4}$$

where $Re = \rho v d/\mu$ is the Reynolds number of the spherical particle settling in the liquid and μ is the dynamic viscosity of the liquid. The above equation is applicable for $1 \leq Re \leq 100$.

However, in our work the settling particle is a non-spherical equiaxed dendrite. In the absence of wall effects, it can be expected that the drag coefficient is a function of both the Reynolds number and the shape of the equiaxed dendrite.[18] A correlation description for a non-spherical particle has been successfully employed by Haider and Levenspiel,[19] and they established drag coefficient C_{d} from experimental data by considering the Reynolds number Re and the sphericity ψ. Since the calculation of the sphericity ψ of the equiaxed dendrite is a difficult task due to the complex shape of real equiaxed dendrites, the equiaxed dendrite may be simplified as some kind of dendrite envelope, such as spherical and pyramid envelopes, as shown in Fig. 1. The spherical envelope is a sphere circumscribing the equiaxed dendrite, and the pyramid envelope consists of six square-based pyramids placed on the six surfaces of a centered cube, where the distance from the center of the cube to the tip of a pyramid equals the length of primary dendrite arm r_1, and θ is the angle between the primary dendrite arm and the straight line connecting the tips of secondary dendrite arms. The pyramid envelope used in this paper is more form fitting to the equiaxed dendrite when compared with the spherical envelope, as less liquid is contained in the envelope.[11] However, the calculated settling velocity will be slightly faster than that in the real situation because the volume calculated is bigger than that of the real dendrite. But when the densities of solid phase and liquid phase have no big difference, this velocity deviation can be ignored because less liquid is contained in the pyramid envelope.

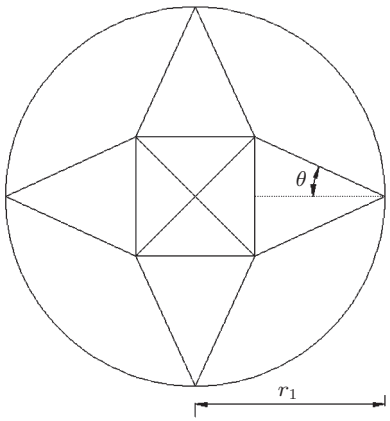


Fig. 1. Schematic diagram of pyramid and spherical envelopes of an equiaxed dendrite.

By this means, the sphericity ψ can be expressed as

$$\psi = \frac{A_{\mathrm{d}}}{A_{\mathrm{s}}}, \tag{5}$$

where A_{d} is the surface area of the dendrite envelope, and A_{s} is the surface area of a spherical particle which has a volume equal to that of the dendrite envelope. According to Fig. 1, the sphericity ψ is calculated as

$$\psi = \frac{6\tan\theta}{\pi g_{\mathrm{s}}^{2/3}(1+\tan\theta)^2\cos\theta}, \tag{6}$$

where g_{s} is the internal solid fraction, which is calculated as

$$g_{\mathrm{s}} = \frac{6}{\pi}\frac{\tan^2\theta}{(1+\tan\theta)^2}. \tag{7}$$

It is known that the confining walls exert an extra retardation force on sediment particles in a cylindrical tube filled with fluid,[20] thus the retardation effect of the tube wall on the drag force should be included in the calculation of the drag coefficient. Fidleris has shown that the wall retardation effect increases with the particle size/tube diameter ratio ($\lambda = d/D$),[21] and the larger the particle size/tube diameter ratio, the stronger the retardation effect of the tube wall on the settling velocity of equiaxed dendrites. Chhabra has investigated the effect of confining walls on the settling velocities of solid particles with different shapes in a stationary liquid,[22] which shows that the wall retardation effect not only is related to the particle size/tube diameter ratio, but also is strongly dependent on the particle shape. It is generally believed that for a

particle morphology with higher complicity, a larger sphericity ψ leads to a stronger retardation effect.

In order to describe the settling behavior of an equiaxed dendrite in a tube, a correction parameter B is introduced, which can be expressed as $B = f(\lambda, \psi)$. By this means, the drag coefficient for an equiaxed dendrite settling in a tube can be updated as

$$C'_{\rm d} = B\left[\frac{24}{Re}\left(1+\frac{3}{16}Re\right)^{1/2}\right]. \tag{8}$$

By substituting Eq. (8) into Eq. (3), the drag force $D'_{\rm r}$ of the equiaxed dendrite settling in a tube can be expressed as

$$D'_{\rm r} = \frac{1}{2}\frac{24}{\left(\frac{\rho v(2r_1)}{\mu}\right)}\left[1+\frac{3}{16}\left(\frac{\rho v(2r_1)}{\mu}\right)\right]^{1/2} \times B\rho\left[\pi\left(g_{\rm s}^{1/3}r_1\right)^2\right]v^2, \tag{9}$$

and is reduced to

$$D'_{\rm r} = 6\pi\mu B\left[1+\frac{3}{16}\left(\frac{\rho v(2r_1)}{\mu}\right)\right]^{1/2} g_{\rm s}^{2/3}r_1 v. \tag{10}$$

Then by substituting Eq. (10) into Eq. (1), the force balance relation is converted to

$$\frac{4}{3}\pi(r_1)^3 g_{\rm s}(\rho_{\rm s}-\rho)g - 6\pi\mu B\left[1+\frac{3}{16}\left(\frac{\rho v(2r_1)}{\mu}\right)\right]^{1/2} g_{\rm s}^{2/3}r_1 v = 0, \tag{11}$$

and is reduced to

$$\frac{2}{9}r_1^2 g_{\rm s}^{1/3}(\rho_{\rm s}-\rho)g = Bv\left(\mu^2+\frac{3}{8}\mu\rho r_1 v\right)^{1/2}. \tag{12}$$

Equation (12) can be used to calculate the settling velocity of an equiaxed dendrite, which has taken into account the retardation effects of both dendrite shape and tube wall and is valid for a moderate Reynolds number region ($1 \le Re \le 100$). However, the correction function B has not been strictly defined. Experiments on an NH_4Cl–H_2O system have been carried out, and size r_1, angle θ, and settling velocity v of NH_4Cl dendrites were measured to validate the function for $B = f(\lambda, \psi)$.

3. Experimental facility and procedure

The present experiments were performed using an NH_4Cl–70wt.%H_2O solution as the experimental transparent alloy solution,[23] the parameters of which are listed in Table 1. A schematic diagram of the experimental setup is shown in Fig. 2, which was composed of the following elements.

Table 1. Material parameters of NH_4Cl–70wt.%H_2O solution.[24]

Properties	Value
Liquidus temperature $T_{\rm L}$/K	307
Mass diffusive of liquid phase $D_{\rm L}/10^9$ m^2·s^{-1}	4.8
Density of liquid phase ρ /10^3 kg·m^{-3}	1.08
Density of solid phase $\rho_{\rm s}/10^3$ kg·m^{-3}	1.53
Dynamic viscosity of liquid phase μ /10^{-3} Pa·s	1.03

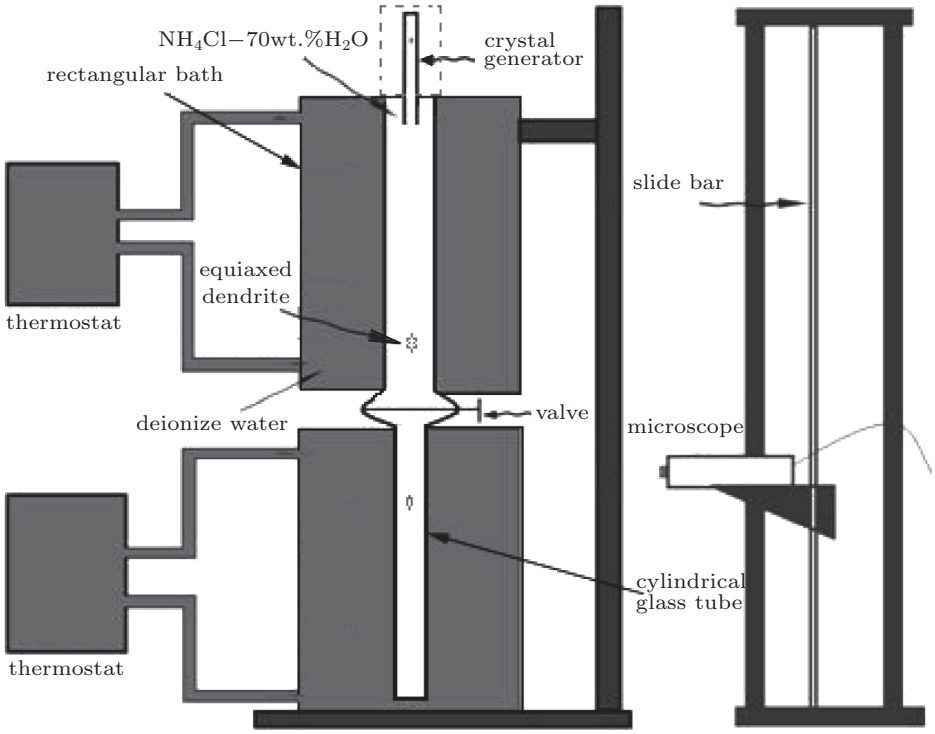


Fig. 2. Schematic diagram of the experimental setup.

A crystal generator filled with the undercooled NH_4Cl–70wt.%H_2O solution was located at the top of an upper cylindrical glass tube, where NH_4Cl small crystal seeds were produced. The upper cylindrical glass tube (2 mm inner diameter and 600 mm height) was also filled with the undercooled NH_4Cl–70wt.%H_2O solution, where the crystal seeds grew to be equiaxed dendrites.

A lower cylindrical glass tube (6 mm inner diameter and 500 mm height) containing the critical-saturated NH_4Cl–70wt.%H_2O solution was joined with the upper cylindrical glass tube by a glass valve, where equiaxed dendrites fell down without any change to morphology.

Two transparent plastic boxes (70 mm×70 mm×600 mm) contained circulating water. The temperature of the circulating water was regulated by two thermostats with accuracy of 0.05 K. Two fall tubes were mounted separately inside the boxes, thus the undercooled and the critical-saturated conditions of NH_4Cl–70wt.%H_2O solution in the two fall tubes were controlled by the temperature of the circulating water.

A video capture device which traveled along the vertical axis parallel to the settling tube was used to record the settling behaviors of the equiaxed dendrites.

NH_4Cl crystal seeds produced in the crystal generator were introduced into the upper fall tube, where the crystal seeds grew into NH_4Cl equiaxed dendrites. The grown-up NH_4Cl equiaxed dendrites fell into the lower fall tube through the valve, and then the video camera travelling along the vertical axis was used to capture the morphology of the settling NH_4Cl equiaxed dendrites.

4. Results and discussion

A typical morphology of an NH_4Cl equiaxed dendrite settling in the saturated solution is shown in Fig. 3. The true values of r_1 and θ were obtained by using the axonometric projection theory to analyze every captured equiaxed dendrite,[25] while the settling velocity v of the equiaxed dendrite was measured directly. Thus g_s, ψ, and Re can be determined, and then the correction function B can be calculated using Eq. (12). Data obtained are shown in Table 2.

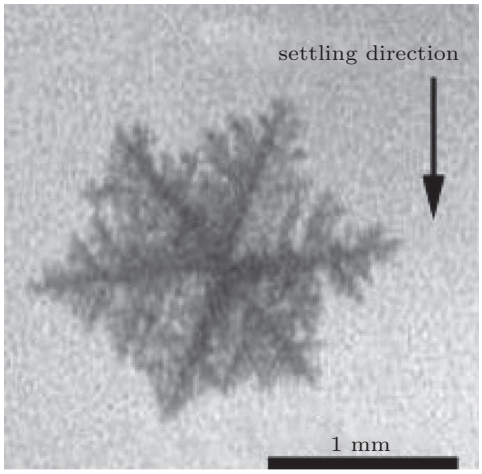


Fig. 3. Typical image of an NH_4Cl equiaxed dendrite settling in the NH_4Cl–70wt.%H_2O solution.

Table 2. Experimental data of NH_4Cl equiaxed dendrites settling in the NH_4Cl–70wt.%H_2O solution.

r_1/mm	v/mm·s^{-1}	Re	θ/(°)	g_s	ψ	λ	$(1-\lambda)\psi$	B
0.49	1.11	1.14	15	0.05	2.39	0.16	2.00	38.92
0.52	1.21	1.32	15	0.05	2.39	0.17	1.98	39.66
0.59	2.07	2.76	16	0.06	2.33	0.20	1.87	33.17
0.62	2.06	2.67	16	0.06	2.33	0.21	1.85	32.46
0.71	3.04	4.51	20	0.08	2.11	0.24	1.61	28.29
0.73	3.15	4.81	20	0.08	2.11	0.24	1.60	28.47
0.75	3.38	5.3	20	0.08	2.11	0.25	1.59	27.32
0.81	3.85	6.53	22	0.10	2.03	0.27	1.48	27.83
0.87	4.23	7.70	22	0.10	2.03	0.29	1.44	27.89
1.01	5.35	11.31	32	0.17	1.74	0.34	1.16	31.91
1.02	5.35	11.42	32	0.17	1.74	0.34	1.15	32.41
1.04	5.50	11.97	32	0.17	1.74	0.35	1.14	32.25
1.05	5.49	12.07	32	0.17	1.74	0.35	1.13	32.85
1.13	6.19	14.64	32	0.17	1.74	0.38	1.08	32.49
1.47	8.71	26.8	32	0.17	1.74	0.49	0.89	33.86
1.50	8.40	26.38	32	0.17	1.74	0.50	0.87	34.44

It can be seen from Table 2 that the measured settling velocity increases with an increase of the size r_1, which is because the corresponding Reynolds number Re increases and the drag coefficient C_d decreases with the increase of the size of the equiaxed dendrite.[26] It is also observed that when the size of equiaxed dendrites r_1 is smaller than 1 mm, the angle

θ increases and the sphericity ψ decreases with the increase of the size due to the coarsening of the secondary dendrite arms. However, when the size of equiaxed dendrite r_1 is larger than 1 mm, these two parameters have constant values, with ψ equal to 1.74 and g_s equal to 0.17. It is because all developed equiaxed dendrites have the same angle θ, which equals to 32°, so g_s and ψ remain unchanged according to Eqs. (7) and 6. By substituting v, ψ, g_s, and r_1 into Eq. (12), the calculated values of B for equiaxed dendrites are determined, as shown in Table 2.

As discussed in Section 2, the retardation effect for a non-spherical particle in a tube is negatively related to λ, and positively related to ψ. The relationship between the retardation effect B and a compound variable of $(1-\lambda)\psi$ is shown in Fig. 4, which shows that the change of correction function B has a parabolic trend along with the increase of $(1-\lambda)\psi$. By fitting the data, an expression can be given as

$$B = 83 - 77(1-\lambda)\psi + 27[(1-\lambda)\psi]^2. \tag{13}$$

It can be seen that in Fig. 4, when $(1-\lambda)\psi$ is larger than 1.4, which corresponds to an equiaxed dendrite with a small size and a varying sphericity, the retardation effect of the tube wall on the drag coefficient is weak, and the retardation effect of the dendrite morphology on the drag coefficient is strong, thus B increases with the increase of $(1-\lambda)\psi$. For the condition of $(1-\lambda)\psi$ less than 1.4, the calculated sphericity is a constant, thus the drag coefficient is only related to the particle size/tube diameter ratio, so B decreases with the increase of $(1-\lambda)\psi$.

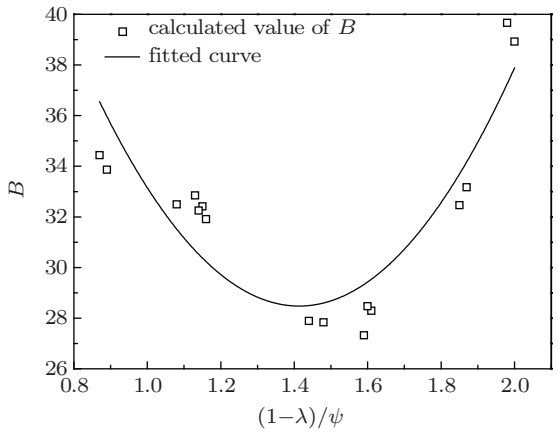


Fig. 4. Relationship between the calculated correction parameter B and $(1-\lambda)\psi$.

Now the internal solid fraction g_s and the sphericity ψ have been experimentally determined by using the pyramids envelope for the equiaxed dendrite, and the correction function B is calculated corresponding to the settling velocity using the identified formula.

In Fig. 5, the settling velocity measured from the experiment and the fitted curve with Eq. (12) are given. In addition, the fitted curve with an assumption of constant drag coefficient is also given, with a relation of

$$v = br_1^{1/2}, \tag{14}$$

where b is a constant. As can be seen from the figure, a significant deviation of Eq. (14) from the experimental results is shown; however, the modified formula (Eq. (12)) considering both the wall and the morphology effects shows good accordance with the experimental results.

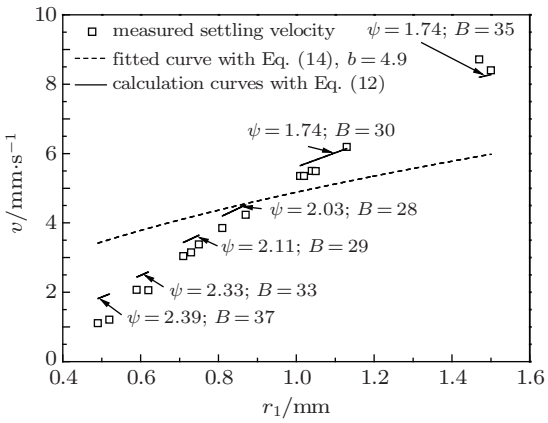


Fig. 5. Measured settling velocities of the equiaxed dendrites and the fitting curves with Eqs. (12) and (14).

5. Conclusion

A calculation formula is established for equiaxed dendrites settling in a tube filled with saturated liquid by including a correction function $B = f(\lambda, \psi)$, which is applicable at the moderate Reynolds number region ($1 \le Re \le 100$) with consideration of both the wall and the morphology effects. The correction function B is determined for experiments performed in an NH_4Cl–H_2O system as $B = 83 - 77(1-\lambda)\psi + 27[(1-\lambda)\psi]^2$. A comparison shows that this formula is reasonably accordant with the experimental results.

References

[1] Biloni H and Chalmers B 1968 *J. Mater. Sci.* **3** 139
[2] Murakami K and Okamoto T 1984 *Materials Science* **18** 103
[3] Ohno A (Translated by Xing Jian-Dong) 1990 *Solidification of Metals: Theory, Practice and Application* (Beijing: China Machine Press) pp. 30–33 (in Chinese)
[4] Li G, Gao Y P, Sun Y N, Chi Z H and Liu R P 2008 *Chin. Phys.* B **17** 3412
[5] Flemings M C 1974 *Metall. Mater. Trans.* B **5** 2121
[6] Yao W J, Yang C, Han X J, Chen M, Wei B B and Guo Z Y 2003 *Acta Phys. Sin.* **52** 448 (in Chinese)
[7] Li Q, Feng W L, Hu X M, Cao Q, Sha D G and Li J M 2008 *Chin. Phys.* B **17** 726
[8] Allen B C and Isserow S 1957 *Actal Metall.* **5** 465
[9] Weinberg F 1984 *Metall. Trans.* B **15B** 479
[10] Yow H N, Pitt M J and Salman A D 2005 *Advanced Powder Technol.* **16** 363
[11] Zakhem R, Weidman P D and de Groh III H C 1992 *Metall. Trans.* A **23A** 2169

[12] de Groh H C, Weidman P D, Zakhem R, Ahuja S and Beckermann C 1993 *Metall. Trans.* B **24** 749
[13] Mirihanage W U and Browne D J 2010 *Comput. Mater. Sci.* **50** 260
[14] Zhang Q Y, Peng Z, He R, Liu R, Lu K Q and Hou M Y 2007 *Acta Phys. Sin.* **56** 4708 (in Chinese)
[15] Chen Z H, Fan B C, Nadine A and Zhou B M 2006 *Chin. Phys. Lett.* **23** 154
[16] Dong P, Feng S D and Zhao Y 2004 *Chin. Phys.* B **13** 434
[17] Olson R B and Wright S J 1990 *Essentials of Engineering Fluid Mechanics* (New York: Harper and Row publishers)
[18] Wu C L and Zhan J M 2005 *Chin. Phys.* B **14** 620
[19] Haider A and Levenspiel 1989 *Powder Technol.* **58** 63
[20] Chhabra R P, Agarwal S and Chaudhary K 2003 *Powder Technol.* **129** 53
[21] Fidleris V and Whitmore R L 1961 *Br. J. Appl. Phys.* **12** 490
[22] Chhabra R P 1995 *Powder Technol.* **85** 83
[23] Shi Y F, Xu Q Y and Liu B C 2011 *Acta Phys. Sin.* **60** 126101 (in Chinese)
[24] Beckermann C and Wang C Y 1996 *Metall. Trans.* A **27A** 2784
[25] Tang R 2001 *Journal of Southeast University* (*Natural Science Edition*) **31** 1 (in Chinese)
[26] Jiménez J A, Madsen O S and Asce M 2003 *J. Waterw. Port C-ASCE* **129** 70